The Journal of Experimental Biology 213, 4092-4098

doi:10.1242/jeb.045088

Characterization of mechanisms for Ca^{2+} and HCO_3^-/CO_3^{2-} acquisition for shell formation in embryos of the freshwater common pond snail *Lymnaea stagnalis*

Sue C. Ebanks[1], Michael J. O'Donnell[2] and Martin Grosell[1]

[1]University of Miami, Rosenstiel School of Marine and Atmospheric Science, Division of Marine Biology and Fisheries, 4600 Rickenbacker Causeway, Miami, FL 33149, USA, [2]Department of Biology, McMaster University, 1280 Main Street West, Hamilton, Ontario L8S 4K1, Canada

Accepted 6 September 2010

SUMMARY

The freshwater common pond snail *Lymnaea stagnalis* produces embryos that complete direct development, hatching as shell-bearing individuals within 10 days despite relatively low ambient calcium and carbonate availability. This development is impaired by removal of ambient total calcium but not by removal of bicarbonate and/or carbonate. In this study we utilized pharmacological agents to target possible acquisition pathways for both Ca^{2+} and accumulation of carbonate in post-metamorphic, shell-laying embryos. Using whole egg mass flux measurements and ion-specific microelectrode analytical techniques, we have demonstrated that carbonic anhydrase-catalyzed hydration of CO_2 is central in the acquisition of both shell-forming ions because it provides the hydrogen ions for an electrogenic vacuolar-type H^+-ATPase that fuels the uptake of Ca^{2+} *via* voltage-dependent Ca^{2+} channels and possibly an electrogenic $Ca^{2+}/1H^+$ exchanger. Additionally, CO_2 hydration provides an endogenous source of HCO_3^-. Thus, hydration of endogenous CO_2 forms HCO_3^- for calcification while hydrogen ions are excreted, contributing to continued Ca^{2+} uptake, as well as creating favorable alkaline internal conditions for calcification. The connections between Ca^{2+} and HCO_3^- acquisition mechanisms that we describe here provide new insight into this efficient, embryonic calcification in freshwater.

Key words: pulmonate snail, metamorphosis, ion-selective microelectrode, ion transport, calcification, embryonic development.

INTRODUCTION

Embryos of the freshwater common pond snail *Lymnaea stagnalis* complete direct development, emerging as shell-bearing hatchlings approximately 10 days post-oviposition in a low-ionic strength, minimally buffered environment. In the absence of ambient total calcium (Ca), they tend to develop at a retarded rate relative to controls but grow and hatch at least as well as controls when reared in carbonate-free water (Ebanks et al., 2010). Although they are provided with maternal stores of calcium and carbonate in the perivitelline fluid and within the gelatinous matrix (tunica interna) of the egg mass, they begin to rely on Ca^{2+} from the surrounding medium as maternal stores in the perivitelline fluid and tunica capsulis become depleted, at approximately day 5 post-oviposition (Ebanks et al., 2010). At this point in embryonic development, embryos increase oxygen consumption and total CO_2 retention (Baldwin, 1935). Metamorphosis and shell formation have been observed for *Lymnaea palustris* (Morrill, 1982), *L. stagnalis* (Ebanks et al., 2010) and another freshwater pulmonate snail *Biomphalaria glabrata* (Bielefeld and Becker, 1991; Marxen et al., 2003). The post-metamorphic Ca^{2+} requirements seem to be met entirely by active uptake, but the carbonate requirements can apparently be accommodated through both uptake and endogenous sources or by endogenous sources exclusively (Ebanks et al., 2010).

The idea of Ca^{2+} uptake in freshwater being by active uptake through Ca^{2+} channels has been presented, studied and reviewed from many angles and by many researchers but mostly in freshwater trout (Flik et al., 1995; Marshall et al., 1992; Perry and Flik, 1988; Shahsavarani and Perry, 2006). An electrochemical gradient for Ca^{2+}, established by basolateral Ca^{2+}-ATPase and Na^+/K^+-ATPase activity, and further facilitated and maintained by an apical, outwardly directed H^+ pump provides the necessary gradient to allow for Ca^{2+} uptake under these conditions (Perry et al., 2003). Hydrogen ions supplied to this pump are mostly from hydration of CO_2. In addition to acid excretion by the H^+ pump, protons can be extruded in exchange for monovalent, as well as divalent, cations *via* Na^+/H^+ exchangers (NHE) by electroneutral or electrogenic exchange (for a review, see Ahearn et al., 2001). Recent work by Okech et al. (Okech et al., 2008) indicated cation exchange for hydrogen ions can be coupled with vacuolar H^+-ATPase (V-ATPase) activity on electrogenic Na^+/H^+ antiporters. A further point of consideration that is important to this study is that $2Na^+/1H^+$ electrogenic exchange, which is apparently unique to invertebrates, can accommodate divalent cations, including Ca^{2+}, in place of the two Na^+ (Ahearn et al., 1994).

Our previous observations of unimpeded growth under HCO_3^--free conditions led to subsequent experiments examining the transport of acid and base equivalents under calcifying, post-metamorphic conditions. We found that the onset of apparent net titratable alkalinity uptake/acid extrusion was concurrent with metamorphosis, the onset of Ca^{2+} uptake and shell formation. Also, Ca^{2+} uptake was significantly greater and apparent net titratable alkalinity uptake/acid extrusion was significantly reduced, but not inhibited, under HCO_3^--free conditions (Ebanks et al., 2010). These findings motivated the series of experiments to determine the possible sources of carbonate for shell formation that are described in this paper.

Considering that carbonic anhydrase-mediated CO_2 hydration produces HCO_3^-, this was a logical starting point. The possibility of endogenous bicarbonate contributing to calcification in the embryos (Baldwin, 1935) and adults (Greenaway, 1971) of this species has been suggested previously in the literature. However, the point of development at which this pathway is activated has not

been studied until recently (Ebanks et al., 2010). Also, the possible role of the proton, resulting from CO_2 hydration and $CaCO_3$ formation, in the acquisition of the essential shell-forming ions by these embryos remains to be evaluated. Therefore, the objectives of this study were to use a pharmacological approach in which flux was measured on the scale of the whole egg mass and the microscale of single eggs to determine the acquisition pathways for shell-forming ions in post-metamorphic embryos of the freshwater common pond snail *Lymnaea stagnalis*. Additionally, we targeted the possible relationship between protons produced by carbonic anhydrase activity and Ca^{2+} uptake. Each of the proposed pathways was evaluated on whole egg mass and at microscale levels when possible.

MATERIALS AND METHODS

Test animals

Egg masses of the common pond snail *Lymnaea stagnalis* (L.) were collected from our laboratory snail culture at 24-h intervals, with the day of collection considered day 0 post-oviposition, for age determination. Embryos were incubated at room temperature (20–22°C) in aerated, dechlorinated Miami-Dade County tap water (Grosell et al., 2007). Whole, intact egg masses were selected and scored for viability in accordance with criteria outlined in Ebanks et al. (Ebanks et al., 2010) prior to use in experimental procedures. With an exception of the niphedipine, verapamil and bafilomycin experiments using the ion-specific microelectrodes, all experiments were completed on intact egg masses as defined in Ebanks et al. (Ebanks et al., 2010).

Whole egg mass flux experiments

Three Ca^{2+} channel blockers were used independently to determine the type and the role of Ca^{2+} channels that may be involved. Nifedipine, which is a voltage-dependent L-type Ca^{2+} channel blocker, was applied as was verapamil, another voltage-dependent L-type Ca^{2+} channel blocker and α1-adrenoceptor antagonist. Lanthanum, an indiscriminate Ca^{2+} channel blocker was also tested. Day 7 egg masses were scored for normal development and placed in Miami-Dade tap water that was either drug-free control (0.1% dimethylsulphoxide; DMSO) or treated for 24 h with either 10 μmol l^{-1} nifedipine (Sigma-Aldrich, St Louis, MO, USA), 10 μmol l^{-1} verapamil hydrochloride (Sigma-Aldrich), 10 μmol l^{-1} La^{3+} or 100 μmol l^{-1} La^{3+} as $LaCl_3$. Initial and final water samples were collected for Ca^{2+} and titratable alkalinity (TA) net flux determinations, which were completed following the protocol for double-endpoint titration described by Ebanks et al. (Ebanks et al., 2010), and are reported in μmol g^{-1} h^{-1}. Considering that carbonate necessary for calcification could be from aquatic sources or endogenous processes (Ebanks et al., 2010), a multi-pronged experimental approach was required. The role of carbonic anhydrase (CA) in the production of endogenous bicarbonate *via* CO_2 hydration was evaluated using a lipophilic carbonic anhydrase inhibitor, ethoxzolamide (ETOX; Sigma-Aldrich), dissolved in DMSO. Controls (0.1% DMSO) and 100 μmol l^{-1} ETOX-exposed egg masses were incubated for 24 h; water samples were taken before and after incubation for Ca^{2+} and TA net flux determinations. In addition to HCO_3^-, CA-catalyzed hydration of CO_2 also produces equal quantities of H^+, which are counterproductive to shell formation and must be excreted to make CO_2 hydration a viable source of CO_3^{2-} for shell formation. Thus we evaluated the role of V-ATPase (a H^+ pump) in the removal of protons and possibly Ca^{2+} uptake, considering that apical Ca^{2+} channels may be driven by an inward-directed electrochemical gradient fueled in part by electrogenic H^+ excretion *via* the H^+ pump. Bafilomycin (Sigma-Aldrich), a proton-pump inhibitor, was dissolved in DMSO for a final concentration of 1 μmol l^{-1} bafilomycin and 0.1% DMSO in each flux chamber. Day-7 egg masses were scored for viability and placed in individual flux chambers for a 24-h incubation, after which we determined net Ca^{2+} and titratable alkalinity flux as described below. Also, because of the potential for direct exchange of Ca^{2+} for H^+ on an apical invertebrate-specific cation/1H^+ exchanger, we completed a 24-h flux experiment in which day-7 egg masses were treated with 100 μmol l^{-1} of the NHE-specific amiloride analogue, ethylisopropylamiloride (EIPA; Sigma-Aldrich) dissolved in a final concentration of 0.1% DMSO.

Analytical procedures for whole egg mass experiments

The procedures for determination of flux rates were in accordance with those outlined by Ebanks et al. (Ebanks et al., 2010). Briefly, samples of pre- and post-flux media were collected for each treatment and Ca^{2+} net flux was determined by using the difference in $[Ca]_{total}$ in initial and final flux media following the 24-h flux. Samples were measured by flame atomic absorption spectrophotometry (Varian SpectrAA220, Mulgrave, Victoria, Australia) and flux rates were calculated from the change in $[Ca]_{total}$, mass of egg mass (g), and elapsed time (h). Net titratable alkalinity flux was calculated from the change in titratable alkalinity as determined by double endpoint titration (Ebanks et al., 2010), mass of egg mass (g) and elapsed time (h). Final values for both Ca^{2+} and titratable alkalinity net flux parameters are presented as μmol g^{-1} h^{-1}.

Ca^{2+}-selective and H^+-selective microelectrodes

Microelectrodes used to measure Ca^{2+} and H^+ gradients in the unstirred layer next to the surface of egg masses and isolated eggs were pulled from unfilamented 1.5 mm borosilicate capillary glass (A-M Systems, Carlsborg, WA, USA), silanized by exposure to dimethyldichlorosilane vapor at 200°C for 60 min and stored over silica gel until use. Ca^{2+}-selective microelectrodes were backfilled with 100 mmol l^{-1} $CaCl_2$ and tip-filled with a 300–500 μm column of Ca^{2+} ionophore I, cocktail A (Fluka, Buchs, Switzerland). H^+-selective microelectrodes were backfilled with a solution of 100 mmol l^{-1} NaCl and 100 mmol l^{-1} sodium citrate at pH 6, then tip-filled with a 300–500 μm column of H^+ ionophore I, cocktail B (Fluka). H^+ microelectrodes calibrated in solutions buffered with 10 mmol l^{-1} Hepes gave Nerstian slopes of 58–60 mV per pH unit.

Ca^{2+} and H^+ fluxes: microscale measurements using the scanning ion electrode technique

Transport of calcium ions or protons into or out of egg masses or isolated eggs produces gradients in Ca^{2+} or H^+ concentration in the unstirred layer adjacent to the surface of the preparation. These gradients can be calculated from the voltages recorded by an ion-selective microelectrode moved between two points within the unstirred layer. Calcium flux can then be calculated from the Ca^{2+} concentration gradients using Fick's law. Measurement of fluxes in this way is the basis of the scanning ion electrode technique (SIET), which allows fluxes to be repeatedly measured in near real-time at sites along the length of an egg mass or an isolated egg (Ebanks et al., 2010).

SIET measurements were made using hardware from Applicable Electronics (Forestdale, MA, USA) and automated scanning electrode technique (ASET) software (version 2.0) from Science Wares Inc. (East Falmouth, MA, USA). Egg masses or isolated eggs were placed in a 35 mm diameter Petri dish filled

with 5 ml of artificial Miami-Dade tap water. Reference electrodes were made from 10 cm lengths of 1.5 mm borosilicate glass capillaries that were bent at a 45 deg angle, 1–2 cm from the end, to facilitate placement in the sample dish. Capillaries were filled with boiling 3 mol l^{-1} KCl in 3% agar and connected to the ground input of the Applicable Electronics amplifier headstage through a Ag/AgCl half cell.

Ca^{2+}-selective microelectrodes for use with SIET were calibrated in 0.1, 1 and 10 mmol l^{-1} Ca. The electrodes showed Nerstian slopes of 28–30 mV per 10-fold change in Ca^{2+} concentration. All scans were performed in artificial Miami-Dade water with a $[Ca]_{total}$ of 400 μmol l^{-1}. The Ca^{2+}-selective microelectrode was initially placed 5–10 μm from the surface of the egg mass or isolated egg. The microelectrode was then moved a further 50 μm away, perpendicular to the egg mass surface. The 'wait' and 'sample' periods at each limit of the 50 μm excursion distance were 4.5 and 0.5 s, respectively. Voltage differences across this excursion distance were measured three times at each of the four to six sites along the surface of each egg mass or isolated egg. There were no significant differences in measurements taken at different sites around the egg masses or eggs, thus measurements were pooled for each sampling period. Voltage differences were corrected for electrode drift measured at a reference site 10–20 mm away from the egg mass. Voltage differences at measurement sites and at reference sites were typically >300 μV and <10 μV, respectively. Voltage differences (ΔV) were converted to the corresponding Ca^{2+} concentration difference by the following equation (Donini and O'Donnell, 2005):

$$\Delta C = C_B \times 10^{(\Delta V/S)} - C_B, \quad (1)$$

where ΔC is the Ca^{2+} concentration difference between the two limits of the excursion distance (in μmol cm^{-3}), C_B is the background Ca^{2+} concentration in the bathing medium, ΔV is the voltage gradient (mV) and S is the slope of the electrode between 0.1 and 1 mmol l^{-1} Ca^{2+}, bracketing the Ca^{2+} concentration in Miami-Dade County tap water. Although ion-selective microelectrodes measure ion activity and not concentration, data can be expressed in terms of concentrations if it is assumed that the ion activity coefficient is the same in calibration and experimental solutions. Expression of data as concentrations aids comparison of Ca^{2+} microelectrode data with those of techniques such as atomic absorption spectrophotometry, which measures Ca^{2+} concentration. Concentrations can be converted to activities by multiplying by the activity coefficient (0.81 for Miami-Dade tap water). The Ca^{2+}-selective microelectrodes used in conjunction with SIET can resolve changes in voltage exceeding the magnitude measured at the reference sites of ~10 μV, corresponding to changes in Ca^{2+} activity of 0.08% in Miami-Dade tap water. Typical signals of 300 μV correspond to changes in Ca^{2+} activity of 2.4%.

Concentration differences were used to determine the Ca^{2+} flux using Fick's law of diffusion:

$$J_{Ca} = D_{Ca}(\Delta C / \Delta X), \quad (2)$$

where J_{Ca} is the net flux in μmol cm^{-2} s^{-1}, D_{Ca} is the diffusion coefficient of Ca^{2+} (1.19×10^{-5} cm^2 s^{-1}), ΔC is the Ca^{2+} concentration gradient and ΔX is the excursion distance between the two points (cm).

Calculation of H^+ fluxes requires knowledge of the buffers that are present (e.g. Donini and O'Donnell, 2005). Ideally, a non-volatile buffer such as Hepes is used. However, because we wished to use the same Miami-Dade tap water as used for the whole egg mass flux experiments, we did not modify the composition of the water and therefore we present H^+ gradients as microelectrode voltage rather than proton flux in the Results.

Statistical analyses

Comparisons were completed using either *t*-test or an ANOVA with contingent significant results evaluated as pairwise comparisons following the Holm–Sidak method after an analysis for whether the datasets were normally distributed. Statements of significance were reserved for those comparisons for which $P<0.05$.

RESULTS

Absolute flux rates of egg masses of similar age varied from batch to batch even under similar conditions. The reason for this variation is unknown but underscores the importance of performing control and treatment experiments simultaneously and on egg masses from the same batch as was done in the present and previous study (Ebanks et al., 2010). Results from our multi-pronged pharmacological approach indicated that voltage-dependent Ca^{2+} channels, H^+-pump activity and Na^+/H^+ antiport function in conjunction with CA activity allow the post-metamorphic embryonic snail to complete calcification and shell formation in freshwater. The two voltage-dependent Ca^{2+} channel blockers had different effectiveness against net Ca^{2+} uptake with nifedipine being the more effective blocker when examined by net Ca^{2+} flux measurements and SIET techniques (Figs 1 and 2). Verapamil did not significantly block net Ca^{2+} transport at 10 μmol l^{-1} but 10 μmol l^{-1} nifedipine did in whole egg mass experiments (Fig. 1). Scanning Ca^{2+}-selective microelectrode analysis showed that both voltage-dependent Ca^{2+}-channel blockers reduced Ca^{2+} transport at 10 μmol l^{-1} but that 100 μmol l^{-1} verapamil completely blocked net Ca^{2+} uptake (Fig. 2). Neither drug influenced net titratable alkalinity flux (data not shown). Lanthanum blocked net Ca^{2+} uptake at 100 μmol l^{-1} but not at 10 μmol l^{-1} in whole egg mass experiments (Fig. 3). There was also a significant increase in apparent net titratable alkalinity uptake/acid extrusion in the presence of 100 μmol La^{3+}(data not shown). Microelectrode experiments revealed a tendency for reduced Ca^{2+} uptake with 100 μmol l^{-1} La^{3+} but just below statistical significance (Fig. 4).

Using 100 μmol l^{-1} ETOX to evaluate the role of CA-catalyzed hydration of CO_2 on whole egg mass flux rates, we observed a significant reduction in both net Ca^{2+} uptake and apparent titratable alkalinity uptake/acid extrusion (Fig. 5). This link between CO_2 hydration and Ca^{2+} uptake led to the testing of the possible role of the apical H^+ pump and Na^+/H^+ exchange by evaluating the inhibitory effects of bafilomycin and EIPA at concentrations of 1 μmol l^{-1} and 100 μmol l^{-1}, respectively, on Ca^{2+} and titratable

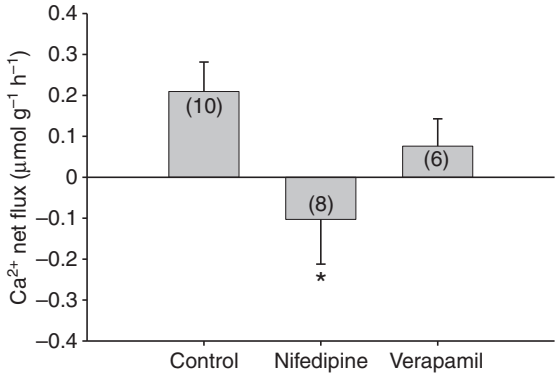

Fig. 1. Net Ca^{2+} flux rate (μmol g^{-1} h^{-1}) under control conditions (0.1% DMSO) and during pharmacological manipulations (10 μmol l^{-1} verapamil or 10 μmol l^{-1} nifedipine). Values are means ± s.e.m. Numbers in parentheses are the numbers of egg masses examined. Ambient $[Ca^{2+}]$=648±7 μmol l^{-1}. *, significantly different from control ($P<0.05$).

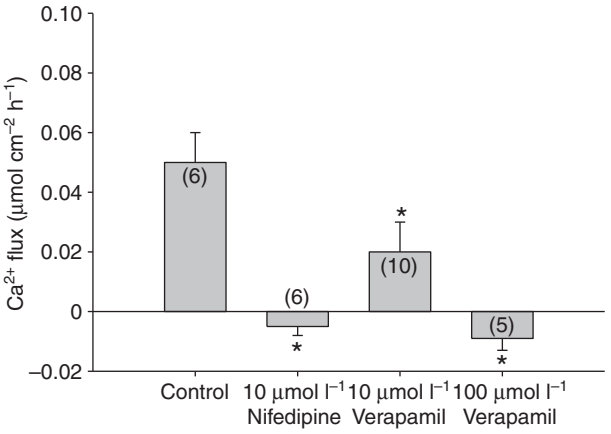

Fig. 2. Results of scanning Ca^{2+}-selective microelectrode analysis of day-9 isolated eggs in control conditions (0.1% DMSO) and during treatment with a voltage-dependent Ca^{2+} channel blocker (nifedipine or verapamil). Values are means ± s.e.m. Numbers in parentheses are the numbers of eggs scanned; five to seven measurements for each egg. *, significant reduction from control values. Ambient $[Ca^{2+}]$=400 μmol l^{-1}.

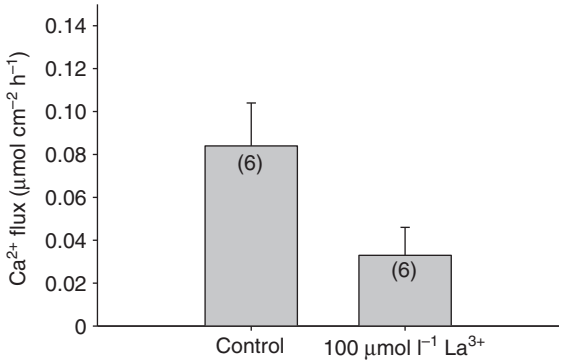

Fig. 4. Results of scanning Ca^{2+}-selective microelectrode analysis of intact day-9 to -10 egg masses in control conditions (0.1% DMSO) and during treatment with a voltage-independent Ca^{2+} channel blocker (100 μmol l^{-1} La^{3+} as $LaCl_3$). Values are means ± s.e.m. Numbers in parentheses are the numbers of eggs scanned; five to ten measurements for each egg. Ambient $[Ca^{2+}]$=400 μmol l^{-1}.

alkalinity transport. Proton-pump inhibition resulted in inhibition of net Ca^{2+} uptake (Fig. 6A) and apparent net titratable alkalinity uptake (equivalent to reduced acid secretion; Fig. 6B). Scanning Ca^{2+}-selective microelectrode measurements revealed that bafilomycin had a significant inhibitory effect of up to 80% on Ca^{2+} transport for post-metamorphic egg masses (data not shown).

Furthermore, and in agreement with whole egg mass fluxes, Ca^{2+} uptake was inhibited in isolated eggs containing later-stage day-11 to -13 embryos, treated with 1 μmol l^{-1} bafilomycin (Fig. 7A) and H^+ gradients were effectively reversed (Fig. 7B) as measured with ion-selective microelectrodes in the unstirred boundary layer. Similar to the bafilomycin treatment, both Ca^{2+} (Fig. 8A) and titratable alkalinity (Fig. 8B) net flux were reversed in whole egg mass fluxes where flux medium was treated with 100 μmol l^{-1} EIPA.

DISCUSSION

The system for Ca^{2+} and carbonate acquisition in the freshwater common pond snail *Lymnaea stagnalis* exhibited sensitivity to several pharmacological agents, which indicate that both Ca^{2+} uptake from the environment as well as endogenous HCO_3^- and/or CO_3^{2-} production work together directly and indirectly for the post-metamorphic embryo to acquire the necessary ions for calcification in freshwater (Fig. 9). Both the dihydropyridine nifedipine and the phenylalkylamine verapamil are known to block L-type Ca^{2+} channels, with nifedipine displaying relatively greater specificity and efficacy to L-type voltage-dependent Ca^{2+} channels (Hagiwara and Byerly, 1981). These compounds inhibit Ca^{2+} channels in some epithelia such as the distal convoluted tubule of the rabbit kidney (Poncet et al., 1992) but not in others, such as the cortical thick ascending limb (Nitschke et al., 1991). The model that we are

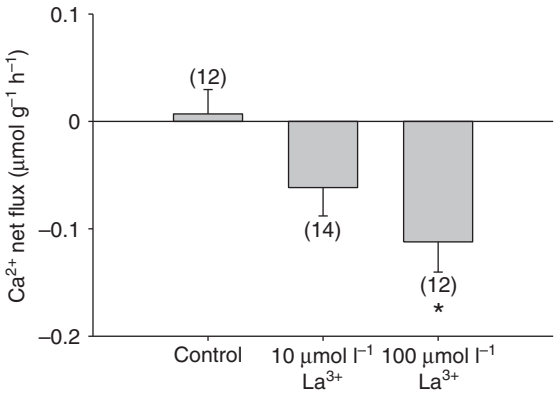

Fig. 3. Net Ca^{2+} flux rates (μmol g^{-1} h^{-1}) in control conditions and during treatment with 10 μmol l^{-1} or 100 μmol l^{-1} La^{3+} as $LaCl_3$. Values are means ± s.e.m. Numbers in parentheses are the numbers of egg masses examined. Ambient $[Ca^{2+}]$=762±0.3 μmol l^{-1}. *, significantly different from control (P<0.05).

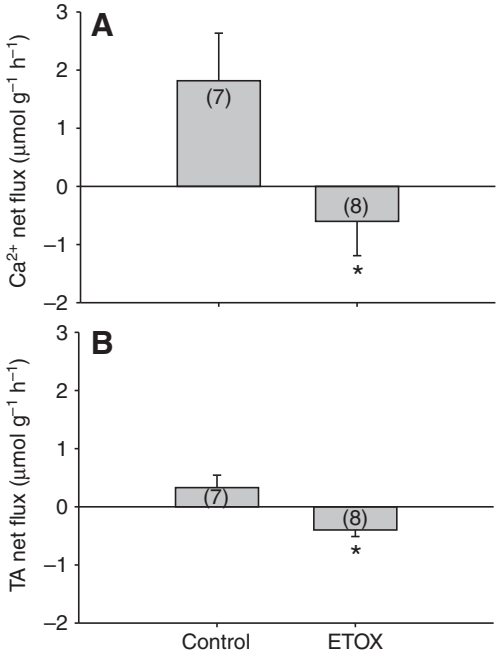

Fig. 5. Comparison of net Ca^{2+} (A) and titratable alkalinity (B) flux rates (μmol g^{-1} h^{-1}) under control conditions (0.1% DMSO) and during pharmacological manipulation with 100 μmol l^{-1} ethoxzolamide (ETOX). Values are means ± s.e.m. Numbers in parentheses are the numbers of egg masses examined. Ambient $[Ca^{2+}]$=1388±79 μmol l^{-1}. *, significantly different from control (P<0.05).

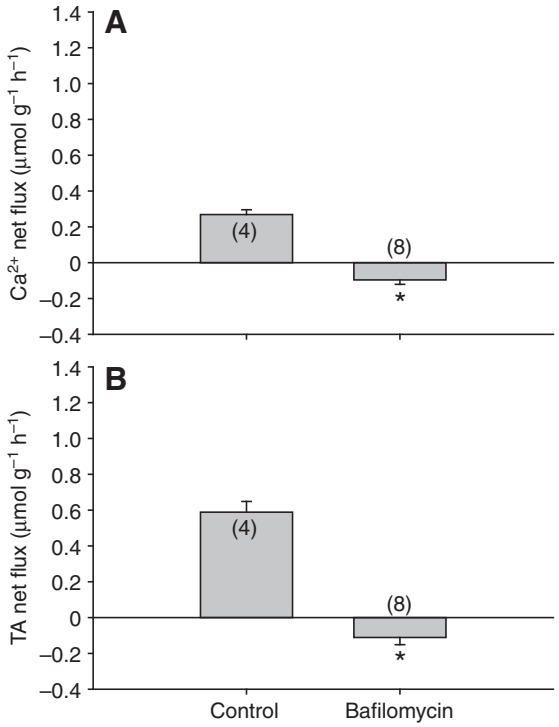

Fig. 6. Comparison of net Ca^{2+} (A) and titratable alkalinity (B) flux rates ($\mu mol\,g^{-1}\,h^{-1}$) under control conditions (0.1% DMSO) and during treatment with $1\,\mu mol\,l^{-1}$ bafilomycin. Values are means ± s.e.m. Numbers in parentheses are the numbers of egg masses examined. Ambient $[Ca^{2+}]$=407±1 $\mu mol\,l^{-1}$. *, significantly different from control (P<0.05).

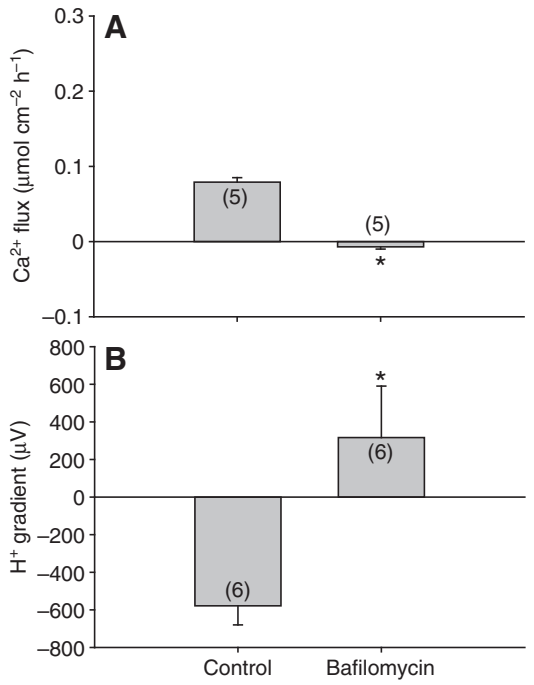

Fig. 7. Comparison of Ca^{2+} flux (A) and H^+ gradients (B) within the unstirred boundary layer of post-metamorphic isolated eggs at day 7 and 8 in control conditions (0.1% DMSO) and during treatment with $1\,\mu mol\,l^{-1}$ bafilomycin. Eggs were scanned using a Ca^{2+}- or H^+-selective microelectrode under control conditions, exposed to drug for 30–60 min, then scanned in drug-treated medium (paired design). Values are means ± s.e.m. Numbers in parentheses are the numbers of eggs examined. Ambient $[Ca^{2+}]$=400 $\mu mol\,l^{-1}$. *, significantly different from control (P<0.05).

proposing here for post-metamorphic embryos compliments findings of Greenaway (Greenaway, 1971) using radioisotopic techniques on adults of the species. In the Greenaway model for adult *Lymnaea*, blood, fresh tissues and shell are identified as the major compartments between which Ca^{2+} is transported (Greenaway, 1971). In times of shell accretion, Ca^{2+} is taken up from the surrounding medium or from food and into the blood for transport to fresh tissues, particularly the mantle, for deposition as $CaCO_3$ after combining with endogenously produced HCO_3^-. Internal production of HCO_3^- by the hydration of CO_2, also produces H^+ ions that are released from the tissues, transported by the blood to excretion sites on the epithelial membrane, and can be exchanged for Ca^{2+}. During times of Ca^{2+} depletion, Ca^{2+} can be acquired from the shell, taken into the soft tissues and blood for transport to sites in need to Ca^{2+} supplement. Thus in adult *Lymnaea*, Ca^{2+} is transported between ambient media, fresh tissues, and shell via the blood (Greenaway, 1971). Considering that these embryos complete direct development, hatching as fully developed snails, it is not surprising to find that the method for acquisition of shell forming ions in embryos apparently is similar to that modeled by Greenaway (Greenaway, 1971).

When applying pharmacological agents that were developed and tested for use on mammals, it is necessary to consider that there may be a reduced degree of specificity of the drug. Additionally, using these chemicals with ion-sensitive microelectrodes can interfere with the sensitivity and function of the electrode. However, our preliminary tests for drug interaction and/or poisoning of the electrode, and the general agreement between results obtained by the two techniques used in the present study, give confidence in the accuracy of our findings. The voltage-dependent Ca^{2+} channel blockers and bafilomycin gave consistent results between whole egg mass net flux measurements and assessment of flux rates by microelectrodes validating the reported observation. With the exception of EIPA, none of the drugs interfered with microelectrode function at the concentrations used in our experiments. Unfortunately, EIPA interfered with both Ca^{2+}- and H^+-selective microelectrodes. EIPA concentrations of $100\,\mu mol\,l^{-1}$ reduced the slope of the Ca^{2+}-selective microelectrodes and caused the H^+ microelectrode voltage to drift. These effects are consistent with a poisoning of the ionophore cocktail by EIPA at $100\,\mu mol\,l^{-1}$. We could not use SIET, therefore, to verify the whole egg mass flux observations that suggested the presence of a cation/H^+ exchanger. Nevertheless, the excellent agreement between observations when made with both techniques is reassuring. L-type voltage-dependent Ca^{2+} channels and an EIPA-sensitive cation exchanger appear to be involved in Ca^{2+} uptake in post-metamorphic embryos (Fig. 9).

In the absence of external HCO_3^-, *Lymnaea stagnalis* embryos grow, form shell, develop normally, and hatch in the same time intervals as controls (Ebanks et al., 2010). These observations point to an internal source of HCO_3^-/CO_3^{2-} for shell formation *via* the hydration of endogenous CO_2. For this hydration reaction to allow for CO_3^{2-} accumulation within the organism and for shell formation, hydrogen ions resulting from the hydration reaction must be eliminated (Fig. 9). We have demonstrated that the enzyme carbonic anhydrase (CA), which facilitates the hydration of endogenous CO_2 is involved in the acquisition of ions for calcification. Also, though

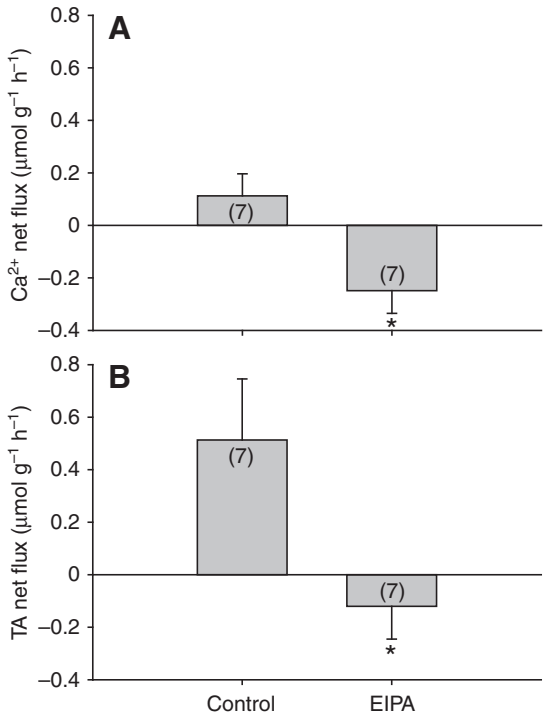

Fig. 8. Comparison of net Ca^{2+} (A) and titratable alkalinity (B) flux rates (μmol g^{-1} h^{-1}) under control conditions (0.1% DMSO) and during treatment with 100 μmol l^{-1} EIPA. Values are means ± s.e.m. Numbers in parentheses are the numbers of egg masses examined. Ambient [Ca^{2+}]=838±16 μmol l^{-1}. *, significantly different from control (P<0.05).

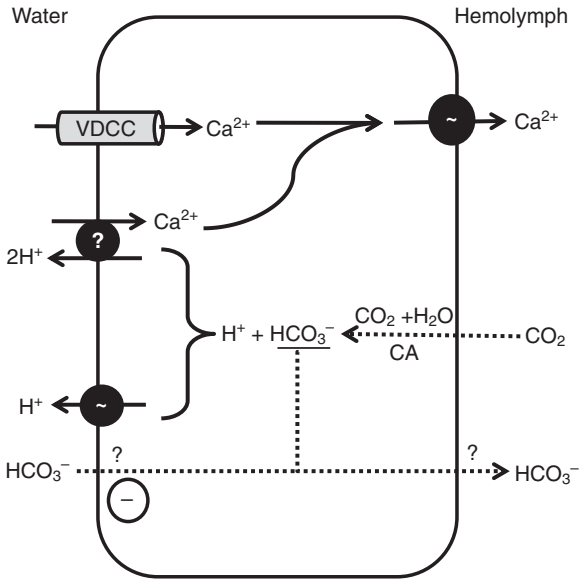

Fig. 9. A schematic diagram of proposed mechanisms for Ca^{2+} and HCO_3^- acquisition in an epithelial cell of a post-metamorphic embryo of the freshwater common pond snail *Lymnaea stagnalis*. H^+ and HCO_3^- are produced by carbonic anhydrase-catalyzed hydration of CO_2. The H^+ ions are excreted *via* the H^+-pump (left-hand closed circle with ~), which contributes to maintenance of an inside negative electrical gradient, driving Ca^{2+} uptake through voltage-dependent Ca^{2+} channels (VDCC). In addition, H^+ excretion facilitates exchange of Ca^{2+} for H^+ on an electrogenic $Ca^{2+}/1H^+$ exchanger that appears to be unique to invertebrates (solid circle with ?) (Greenaway 1971; Okech et al., 2008; Ahearn et al., 1994; Ahearn et al., 2001). There is also evidence that uptake of HCO_3^-, when available in the water, occurs *via* an undefined pathway (Ebanks et al., 2010). It is assumed that a basolateral Ca^{2+}-ATPase is responsible for transport of Ca^{2+} across the basolateral membrane (right-hand closed circle with ~) and that HCO_3^- ions are passed across the basolateral membrane to the extracellular fluid or hemolymph. See text for further details.

developing snails show an apparent net uptake of Ca^{2+} and HCO_3^- equivalents, the movement of acid–base equivalents is in reality a combination of acid secretion and base uptake, because it persists, although at reduced rates, in absence of ambient HCO_3^- (Ebanks et al., 2010). Our SIET measurements of H^+ gradients further confirm the role of H^+ excretion.

The effects of CA inhibition indicated a direct role for CA in carbonate production in post-metamorphic embryos but also points to an indirect role in Ca^{2+} acquisition that is revealed when considered in conjunction with the bafilomycin A_1 results. Bafilomycin inhibits V-ATPase activity, which has been found to be ubiquitous among eukaryotes (Harvey, 1992; Finbow and Harrison, 1997; Harvey et al., 1998). This includes invertebrates and more directly related to our model species, calcifying organisms such as blue crabs (Cameron and Wood, 1985). This enzyme has also been characterized in tissues of freshwater bivalves *Anodonta cygnea* (Machado et al., 1990; da Costa et al., 1999; Oliveira et al., 2004), *Unio complanatus* (Hudson, 1993) and *Nucella lamellosa* (Clelland and Saleuddin, 2000). The connection between H^+-pump activity and cation uptake has been demonstrated in epithelia of a variety of species (Harvey et al., 1998), including Ca^{2+} uptake by post-moult blue crabs *Callinectes sapidus* (Cameron and Wood, 1985; Neufeld and Cameron, 1992). There have also been reviews on the presence of this pathway in crustaceans (Neufeld and Cameron, 1993). Furthermore, H^+-pump-driven active cation uptake has been documented in adults of this species (Ebanks and Grosell, 2008) as well as in several other freshwater species including carp (Fenwick et al., 1999), tilapia (Fenwick et al., 1999) and trout (Bury and Wood, 1999; Grosell and Wood, 2002; Lin and Randall, 1991). Thus inhibition of Ca^{2+} uptake in the presence of the V-ATPase inhibitor, bafilomycin, in developing snail embryos is persistent across later time points (up to 80% reduction in post-metamorphic Ca^{2+} uptake) and appears to be consistent with investigations in other species. Thus the H^+ pump plays a significant role in Ca^{2+} flux in post-metamorphic stages. By electrogenic excretion of H^+ ions, the electrical potential across the apical membrane, and thereby the electrochemical gradient for Ca^{2+} uptake is maintained. In addition, the observations of reduced acid excretion and Ca^{2+} uptake in the presence of the specific Na^+/H^+ exchange inhibitor, EIPA, points to an even more direct coupling of H^+ extrusion to Ca^{2+} uptake. However, Hudson found no effect of 1 mmol l^{-1} amiloride or Na^+-depleted solutions on acid secretion in Ussing-type chamber experiments on mantle epithelia of *U. complanatus* (Hudson, 1993). EIPA was not included in the study, but there was no detectable coupling between a proxy for acid secretion, cAMP-dependent short-circuit current (I_{SC}) (Machado et al., 1990), and unidirectional Na^+, K^+, Ca^{2+} or Cl^- fluxes in the same species (Hudson, 1993). Nevertheless, our data suggest the presence and involvement of a Ca^{2+}/H^+ exchanger in *L. stagnalis*. It is interesting to note that electrogenic Ca^{2+}/H^+ exchange would be facilitated by parallel electrogenic H^+ extrusion by the H^+ pump.

Taken together, our results suggest that through the use of the ionic products of CO_2 hydration, H^+ and HCO_3^-, the high Ca^{2+} and carbonate demands for shell formation in freshwater are met and maintained with notable efficiency. The higher the rate of CO_2

hydration, the higher the rate of HCO_3^- formation, and the higher the amount of H^+ excretion by the proton pumps and/or cation exchange, which in turn provides for Ca^{2+} uptake. Inhibition of CA activity leads to inhibition of transport of both shell-forming ions. Admittedly, inhibition of the ability to hydrate respiratory CO_2 can have broader impacts on the physiological level. However, when the results of CA inhibition are taken in conjunction with the response to H^+ pump and NHE inhibition as well as the ability of the embryos to develop in HCO_3^--free conditions (Ebanks et al., 2010), there is substantial evidence that endogenously produced carbonate can be an exclusive carbonate source for these post-metamorphic embryos. A further point to consider is that in addition to protons produced from hydration of metabolic CO_2, H^+ ions are liberated by the calcification process ($HCO_3^-+Ca^{2+}\rightarrow CaCO_3+H^+$) adding to the need for acid secretion by these animals. By coupling Ca^{2+} uptake and HCO_3^- production with the generation of inside alkaline conditions via H^+ extrusion, the conditions for calcification within the egg and egg mass are enhanced. Furthermore, the depletion of Ca^{2+} within the perivitelline fluid and gelatinous matrix (tunica interna) between the eggs to levels below water concentrations during later embryonic stages (Ebanks et al., 2010) creates an inward Ca^{2+} gradient and thus can enhance the influx of Ca^{2+} from the surrounding water while decreasing the energy required for ion uptake.

Conclusions

Acquisition of the necessary Ca^{2+} and carbonate for calcification by embryos of the freshwater common pond snail *Lymnaea stagnalis* are intricately intertwined. These embryos take up Ca^{2+} from ambient media after maternal stores in the perivitelline fluid have been depleted; but they also directly utilize endogenously produced bicarbonate from the CA-catalyzed hydration of CO_2. Protons generated from CO_2 hydration are excreted, which fuels continued Ca^{2+} uptake and allows for accumulation of bicarbonate and maintenance of alkaline internal conditions that are favorable for calcification. With endogenous production of HCO_3^- for calcification perpetuating continued Ca^{2+} uptake, these embryos are capable of efficient calcification under low ionic strength conditions.

With global climate change, studies are necessary to determine how ambient pH and bicarbonate buffering affect the ability of these freshwater snails to calcify. Furthermore, evaluating the extent to which acid secretion rather than base uptake is the basis for calcification in other freshwater as well as marine calcifiers offers an exciting area for comparative studies.

LIST OF ABBREVIATIONS

CA	carbonic anhydrase
EIPA	ethylisopropylamiloride ($C_{11}H_{18}ClN_7O$)
ETOX	ethoxzolamide ($C_9H_{10}N_2O_3S_2$)
NHE	Na^+/H^+ exchanger

ACKNOWLEDGEMENTS

S.C.E. appreciates the technical assistance and hospitality of Andrea Kocmarek and Erin Leonard of McMaster University offered during her visit to the O'Donnell laboratory. This research was funded in part by the NOAA Educational Partnership Program, Environmental Cooperative Science Center and the RSMAS Marine Science Graduate Student Organization Student Travel Fund.

REFERENCES

Ahearn, G. A., Zhuang, Z., Duerr, J. and Pennington, V. (1994). Role of invertebrate electrogenic $2Na^+/1H^+$ antiporter in monovalent and divalent cation transport. *J. Exp. Biol.* **196**, 319-335.

Ahearn, G. A., Mandal, P. K. and Mandal, A. (2001). Biology of the $2Na^{1+}/1H^{1+}$ antiporter in invertebrates. *J. Exp. Zool.* **289**, 232-244.

Baldwin, E. (1935). The energy sources in ontogenesis. VIII. The respiratory quotient of developing gastropod eggs. *J. Exp. Biol.* **12**, 27-35.

Bielefeld, U. and Becker, W. (1991). Embryonic development of the shell in *Biompharia glabrata* (Say). *Int. J. Dev. Biol.* **35**, 121-131.

Bury, N. R. and Wood, C. M. (1999). Mechanism of branchial apical silver uptake by rainbow trout is via the proton-coupled Na^+ channel. *Am. J. Physiol. Regul. Integr. Comp. Physiol.* **277**, R1385-R1391.

Cameron, J. N. and Wood, C. M. (1985). Apparent H^+ excretion and CO_2 dynamics accompanying carapace mineralization in the blue crab (*Callinectes sapadus*) following moulting. *J. Exp. Biol.* **114**, 181-196.

Clelland, E. S. and Saleuddin, A. S. M. (2000). Vacuolar-type ATPase in the accessory boring organ of *Nucella lamellosa* (Gmelin) (Mollusca: Gastropoda): Role in shell penetration. *Biol. Bull.* **198**, 272-283.

da Costa, A. R., Oliveira, P. F., Barrias, C. and Ferreira, H. G. (1999). Identification of a V-type proton pump in the outer mantle epithelium of *Anodonta cygnea*. *Comp. Biochem. Physiol.* **123A**, 337-342.

Donini, A. and O'Donnell, M. J. (2005). Analysis of Na^+, Cl^-, K^+, H^+ and NH_4^+ concentration gradients adjacent to the surface of anal papillae of the mosquito *Aedes aegypti*: application of self-referencing ion-selective microelectrodes. *J. Exp. Biol.* **208**, 603-610.

Ebanks, S. C. and Grosell, M. (2008). Fluid and osmolyte recovery in the common pond snail *Lymnaea stagnalis* following full-body withdrawal. *J. Exp. Biol.* **211**, 327-336.

Ebanks, S. C., O'Donnell, M. J. and Grosell, M. (2010). Acquisition of Ca^{2+} and carbonate for shell formation in embryos of the common pond snail *Lymnaea stagnalis*. *J. Comp. Physiol. B* **180**, 953-965.

Fenwick, J. C., Wendelaar Bonga, S. E. and Flik, G. (1999). In vivo bafilomycin-sensitive $Na(^+)$ uptake in young freshwater fish. *J. Exp. Biol.* **202**, 3659-3666.

Finbow, M. E. and Harrison, M. A. (1997). The vacuolar H^+-ATPase: a universal proton pump of eukaryotes. *Biochem. J.* **324**, 697-712.

Flik, G., Verbost, P. M. and Wendelaar Bonga, S. E. (1995). Calcium transport processes in fishes. In *Cellular and molecular approaches to fish ionic regulation* (ed. C. M. Wood and T. J. Shuttleworth), pp. 317-336. New York: Academic Press.

Greenaway, P. (1971). Calcium regulation in the freshwater mollusc *Limnaea stagnalis* (L.) (Gastropoda: Pulmonata). II. Calcium movements between internal calcium compartments. *J. Exp. Biol.* **54**, 609-620.

Grosell, M. and Wood, C. M. (2002). Copper uptake across rainbow trout gills: mechanisms of apical entry. *J. Exp. Biol.* **205**, 1179-1188.

Grosell, M., Blanchard, J., Brix, K. V. and Gerdes, R. (2007). Physiology is pivotal for interactions between salinity and acute copper toxicity to fish and invertebrates. *Aquat. Toxicol.* **84**, 162-172.

Hagiwara, S. and Byerly, L. (1981). Calcium channel. *Annu. Rev. Neurosci.* **4**, 69-125.

Harvey, W. R. (1992). Physiology of V-ATPases. *J. Exp. Biol.* **172**, 1-17.

Harvey, W. R., Maddrell, S. H. P., Telfer, W. H. and Wieczorek, H. (1998). H^+ V-ATPases energize plasma membranes for secretion and absorption of ions and fluids. *Amer. Zool.* **38**, 426-441.

Hudson, R. L. (1993). Bafilomycin-sensitive acid secretion by mantle epithelium of the freshwater clam, *Unio complanatus*. *Am. J. Physiol. Regul. Integr. Comp. Physiol.* **264**, R946-R951.

Lin, H. and Randall, D. (1991). Evidence for the presence of an electrogenic proton pump on the trout gill epithelium. *J. Exp. Biol.* **161**, 119-134.

Machado, J., Ferreira, K. G., Ferreira, H. G. and Fernandes, P. L. (1990). The acid-base balance of the outer mantle epithelium of *Anodonta cygnea*. *J. Exp. Biol.* **150**, 159-169.

Marshall, W., Bryson, S. and Wood, C. (1992). Calcium transport by isolated skin of rainbow trout. *J. Exp. Biol.* **166**, 297-316.

Marxen, J. C., Becker, W., Finke, D., Hasse, B. and Epple, M. (2003). Early mineralization in *Biomphalaria glabrata*: Microscopic and structural results. *J. Mollus. Stud.* **69**, 113-121.

Morrill, J. B. (1982). Development of the pulmonate gastropod, *Lymnaea*. In *Developmental Biology of Freshwater Invertebrates* (eds. W. Harrison and R. F. Cowdon), pp. 399-483. New York: Alan R. Liss.

Neufeld, D. S. and Cameron, J. N. (1992). Postmoult uptake of calcium by the blue crab (*Callinectes sapadus*) in water of low salinity. *J. Exp. Biol.* **171**, 283-299.

Neufeld, D. S. and Cameron, J. N. (1993). Transepithelial movement of calcium in crustaceans. *J. Exp. Biol.* **184**, 1-16.

Nitschke, R., Fröbe, U. and Greger, R. (1991). Antidiuretic hormone acts via V_1 receptors on intracellular calcium in the isolated perfused rabbit cortical thick ascending limb. *Pflügers Arch.* **417**, 622-632.

Okech, B. A., Boudko, D. Y., Linser, P. J. and Harvey, W. R. (2008). Cationic pathway of pH regulation in larvae of *Anopheles gambiae*. *J. Exp. Biol.* **211**, 957-968.

Oliveira, P. F., Lopes, I. A., Barrias, C. and Rebelo da Costa, A. M. (2004). H^+-ATPase of crude homogenate of the outer mantle epithelium of *Anodonta cygnea*. *Comp. Biochem. Physiol.* **139A**, 425-432.

Perry, S. F. and Flik, G. (1988). Characterization of branchial transepithelial calcium fluxes in freshwater trout, *Salmo gairdneri*. *Am J. Physiol. Regul. Integr. Comp. Physiol.* **254**, R491-R498.

Perry, S. F., Shahsavarani, A., Georgalis, T., Bayaa, M., Furimsky, M. and Thomas, S. L. Y. (2003). Channels, pumps, and exchangers in the gill and kidney of freshwater fishes: Their role in ionic and acid-base regulation. *J. Exp. Zool.* **300A**, 53-62.

Poncet, V., Merot, J. and Poujeol, P. (1992). A calcium-permeable channel in the apical membrane of primary cultures of the rabbit distal bright convoluted tubule. *Pflügers Arch.* **422**, 112-119.

Shahsavarani, A. and Perry, S. F. (2006). Hormonal and environmental regulation of epithelial calcium channel in gill of rainbow trout (*Oncorhynchus mykiss*). *Am J. Physiol. Regul. Integr. Comp. Physiol.* **291**, R1490-R1498.